

Understanding of hopping matrix for 2D materials taking 2D honeycomb and square lattices as study cases

Maher Ahmed

Department of Physics and Astronomy,

University of Western Ontario, London ON N6A 3K7, Canada and

Physics Department, Faculty of Science,

*Ain Shams University, Abbsai, Cairo, Egypt**

Abstract

In this work, a trial understanding for the physics underling the construction of exchange (hopping) matrix \mathbf{E} in Heisenberg model (tight binding model) for 2D materials is done. It is found that the \mathbf{E} matrix describes the particles exchange flow under short range (nearest neighbor) hopping interaction which is effected by the lattice geometry. This understanding is then used to explain the dispersion relations for the 2D honeycomb lattice with zigzag and armchair edges obtained for graphene nanoribbons and magnetic stripes. It is found that the particle flow by hopping in the zigzag nanoribbons is a translation flow and shows $\cos^2(q_x a)$ dependance while it is a rotational flow in the armchair nanoribbons. At $q_x a/\pi = 0.5$, the particles flow in the edge sites of zigzag nanoribbons with dependance of $\cos^2(q_x a)$ is equal to zero. At the same time there is no vertical hopping in those edge sites which lead to the appearance of peculiar zigzag flat localized edge states.

* mahmed62@uwo.ca

I. INTRODUCTION

It is shown in [1–3] that the physics of the Heisenberg Hamiltonian system and tight binding Hamiltonian system for 2D honeycomb armchair and zigzag nanoribbons shown in Figure 1 are nearly equivalent which is a reflection of their equivalent from geometrical and topological point of view, as both system represent an exchange (a hopping) flow of particles, electrons (fermions) in graphene case and magnons (bosons) in magnetic case, under short range interaction (nearest neighbor exchange J_{ij} for magnetic excitations and nearest neighbor hopping t_{ij} for electronic excitations) through the same 2D honeycomb lattice.

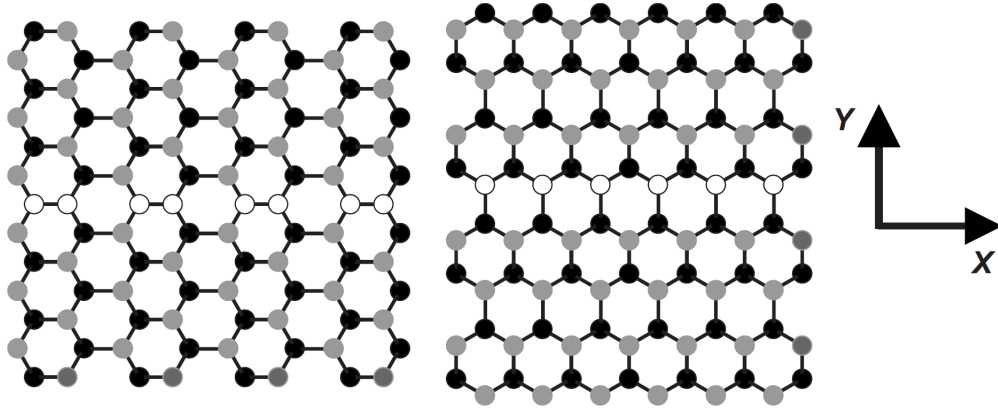


FIG. 1. Armchair (left) and zigzag (right) 2D Heisenberg ferromagnetic dots honeycomb stripes in xy -plane, where black (gray) dots are the sublattice A(B) with a line of impurities (white dots) in the middle of the sheet, and with average spin S alignment in z direction. The stripes are finite in y direction with N rows ($n = 1, \dots, N$) and they are infinite in the x direction. Figure taken from [3].

All the important geometrical and topological information that effect this exchange (hopping) flow for both systems are encoded in the following \mathbf{E} matrix

$$\mathbf{E} = \begin{bmatrix} \alpha I_N & T(q_x) \\ T^*(q_x) & \alpha I_N \end{bmatrix}, \quad (1)$$

here, $T(q_x)$ is the exchange matrix, which depends on the orientation of the ribbon and is given by

$$\begin{pmatrix} \varepsilon & \beta & 0 & 0 & \cdots \\ \beta & \varepsilon & \gamma & 0 & \cdots \\ 0 & \gamma & \varepsilon & \beta & \cdots \\ 0 & 0 & \beta & \varepsilon & \cdots \\ \vdots & \vdots & \vdots & \vdots & \ddots \end{pmatrix}, \quad (2)$$

where the parameters ε , γ , and β depend on the stripe edge geometry and are given in Table I.

TABLE I. Nearest neighbor exchange matrix elements for 2D magnetic honeycomb lattice

Parameter	Zigzag	Armchair
ε	0	$\frac{SJ}{2}e^{-iq_x a}$
β	$SJ \cos(\sqrt{3}q_x a/2)$	$\frac{SJ}{2}e^{iq_x a/2}$
γ	$\frac{SJ}{2}$	$\frac{SJ}{2}e^{iq_x a/2}$

It turns out that allowed exchange (hopping) flow modes inside the lattice are the eigenvalues of that matrix [1–3]

$$\omega(q_x) \begin{bmatrix} a_n \\ b_n \end{bmatrix} = \begin{bmatrix} \alpha I_N & T(q_x) \\ T^*(q_x) & \alpha I_N \end{bmatrix} \begin{bmatrix} a_n \\ b_n \end{bmatrix}, \quad (3)$$

where a_n and b_n are the annihilation boson operators for the 2D honeycomb sublattices A and B respectively [4], q_x is wavevector along the x axis which is the translation symmetry direction of the nanoribbons, and $\omega(q_x)$ are the frequencies of the spin wave modes.

The \mathbf{E} matrix describes in general two allowed directions for particles exchange (hopping) flow: one along the direction of translation symmetry for the 2D lattices, and the other along the vertical to that translation symmetry direction. The main effect of particles exchange (hopping) flow along the direction of translation symmetry for the 2D lattices is the changing in the energy of allowed propagation modes due to the 2D lattice symmetry encoded as a function in the particles momentum component along that direction of translation symmetry. The main effect of vertical particles exchange (hopping) flow in the 2D lattice stripes and nanoribbons is the quantization of allowed modes due to the quantum confinement effect for particles motion in the vertical direction

to translation symmetry axis. This vertical particles exchange (hopping) flow is independent of the particles momentum component in the direction of translation symmetry for the 2D lattices.

II. UNDERSTANDING EXCHANGE MATRIX

The \mathbf{E} matrix has two sub matrixes components: αI_N and $T(q_x)$. The first sub matrix component αI_N represents insite energy value in the lattice, which in turn represent each sites potential energy for exchange flow of particles inside the lattice. When all sites have the same potential energy value, (i.e. perfect and impurity free lattice), the resistance for exchange flow between the lattice sites is nearly zero and consequently the particles flow form a perfect fluid, which can be seen in graphene [5]. Introducing any change for insite energy in the lattice for example the effects due to change edge uniaxial anisotropy studied in [2] resulting changing in edges insite energy which break the flow symmetry in the lattice as it is seen in magnetic stripes and graphene nanoribbon [6].

The second sub matrix component $T(q_x)$ represents the effect of lattice geometry in the particles exchange flow (propagation) inside the lattice under nearest neighbor exchange (hopping) which depends on the edge configuration as zigzag or armchair [7]. To further clarify the above meaning of the $T(q_x)$ matrix, a closer examination of its derivation in [1–3] is needed. Its derivation starts from the following exchange sum

$$\gamma(q_x) = \frac{1}{2} S \sum_v J_{i,j} e^{-i\mathbf{q}_x \cdot (\mathbf{r}_i - \mathbf{r}_j)}. \quad (4)$$

The sum for the exchange terms $J_{i,j}$ is taken to be over all v nearest neighbors in the lattice which depends on the edge configuration as zigzag or armchair for the stripe. For the armchair configuration, the exchange sum gives the following amplitude factors $\gamma_{nn'}(q_x)$

$$\gamma_{nn'}(q_x) = \frac{1}{2} S J \left[\exp(iq_x a) \delta_{n',n} + \exp\left(i\frac{1}{2}q_x a\right) \delta_{n',n\pm 1} \right], \quad (5)$$

while for the zigzag case it gives

$$\gamma_{nn'}(q_x) = \frac{1}{2} S J \left[2 \cos\left(\frac{\sqrt{3}}{2}q_x a\right) \delta_{n',n\pm 1} + \delta_{n',n\mp 1} \right]. \quad (6)$$

The \pm sign depends on the sublattice since the sites line alternates from A and B.

The exchange sum represents the directed component of exchange flow to each nearest neighbor with respect to the direction of translation symmetry of the stripe described by Fourier transform.

Applying the exchange sum 4 to each armchair and zigzag site with its nearest neighbor connections in 2D honeycomb lattice in the direction of translation symmetry of the stripe as shown in Figure 2 results in the amplitude factors 5 and 6, which are the elements of exchange matrix $T(q_x)$. Each element in this matrix is the product of exchange strength and geometrical amplitude as seen in Table I, which expressing the modulation of nearest neighbor exchange strength due to the flow topology inside the lattice which depend on both the wavevector (i.e the momentum) of the particle and the edge configuration as zigzag or armchair.

The matrix elements consist of three types: the diagonal element representing the nearest neighbor exchange between sites lies in the same line along the direction of translation symmetry of the stripe, after diagonal element representing the nearest neighbor exchange between the sites at the same line and next line in the lattice sites, and before diagonal element representing the nearest neighbor exchange between the sites in same line and upper line in the lattice sites.

III. APPLYING EXCHANGE MATRIX TO 2D HONEYCOMB LATTICE

Using the above explanation for the elements of exchange matrix $T(q_x)$ and the Table I, we can now understand the exchange (the hopping) flow of particles in 2D Honeycomb Lattice. Beginning by the zigzag stripes, the diagonal elements is zero since the sites in the same line in zigzag stripe are not nearest neighbor and therefore no exchange flow through that line. For up and under diagonal elements, the alternates between A and B sites lines create alternates parallel connected zigzag lines with vertical connections, which clear from Figures 1 and 2.

The element β represents the exchange flow in the parallel zigzag lines along the translation symmetry of the zigzag stripe, where the real term $[2 \cos(\sqrt{3}q_x a/2)]$ comes from the sum of $[\exp(-i\sqrt{3}q_x a/2) + \exp(i\sqrt{3}q_x a/2)]$ which reflect the ability to move nearly linear parallel to the translation symmetry direction, which modulate the exchange strength according to the particle momentum q_x . The element $\gamma = (SJ/2)$ represents the exchange flow in vertical connections between the parallel zigzag lines and perpendicular to the translation symmetry of the zigzag stripe, the term comes from $[(SJ/2) \exp(-i\mathbf{q}_x \cdot (\mathbf{r}_i - \mathbf{r}_j))]$, which is equal to $(SJ/2)$ since $(\mathbf{r}_i - \mathbf{r}_j)$ is perpendicular to q_x for vertical sites which leads the exponential term to be equal to 1, and therefore the exchange strength in the vertical direction is constant and independent on q_x .

The particle in any interior site in the zigzag stripe will be under two competitive exchange (hopping) force with different strength: one through a zigzag line along the translation symmetry

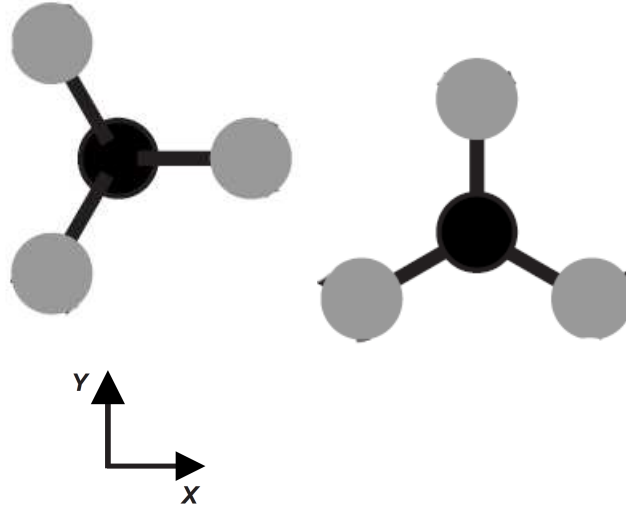


FIG. 2. Nearest neighbor connections for a site in 2D honeycomb lattice in the direction of translation symmetry of the stripe. The Right is the armchair site while the left is the zigzag site

of the stripe and the other through vertical connections between the parallel zigzag lines, the main factor that detriment which direction the particle has high probability to flow is its momentum in translation symmetry direction q_x . The exchange (hopping) strength in the zigzag lines direction is much larger than the exchange strength in the noncontinuous vertical lines direction in most of q_x values and the particle has high probability to flow in zigzag lines. The direction of flow in upper edge is x direction while in the lower edge is $-x$ direction (see Figure 3a) this is due to the reversing in the zigzag lines sequence between up and lower edges, i.e. AB, BA, AB,...AB, BA. This behavior is displayed in the determinant condition of equation 3 as a dependence on the exchange matrix squared $T^2(q_x)$ [8] which leads to $\cos^2(\sqrt{3}q_x a/2)$ dependance of the modes dispersions of zigzag stripe. When particle momentum q_x is zero which verify the conditions $q_x a = 0$ the exchange (hopping) strength in the zigzag lines direction is nearly double exchange strength in noncontinuous vertical direction and the particle has high probability to flow in zigzag lines which shown as maximum (minimum) energy in the dispersion relations. As particle momentum reaches the value that verify the condition $q_x a/\pi = 0.5$ the exchange (hopping) strength in the zigzag line direction is nearly zero and the particle under only exchange in noncontinuous vertical direction. Therefore the particle has high probability to flow in noncontinuous vertical line which reflected in the mode dispersion of zigzag stripe a node point. As the particle momentum increases the exchange flow direction through the stripe and its edge is reversed and begin to increase again as

a reflection for $\cos^2(\sqrt{3}q_x a/2)$ dependance of the modes dispersions of zigzag stripe, as q_x reach π the modes dispersions reach the maximum (minimum) energy.

The situation is completely different for a particle in any edge site in the zigzag stripe because the edge site has coordination number equal to either two or one and consequently the particle in the edge site will be under only one exchange (hopping) force. If the edge site has coordination number equal to two, the particle in the edge site will be under only the exchange (hopping) strength in the zigzag line direction and the particle has high probability to flow in the edge zigzag line, while the exchange (hopping) strength dependance on the particle momentum q_x is effecting the particle flow in the zigzag line in this case since no competition with missing vertical exchange (hopping). Only when the particle momentum reaches near the value that verify the condition $q_x a/\pi = 0.5$ the exchange (hopping) strength in the zigzag line direction is nearly zero, and the particle become localized in the edge sites, which create the edge localized states. The flatness of edge states coming from the small range of q_x around $q_x a/\pi = 0.5$ where the exchange (hopping) strength in the zigzag line direction at edge sites is nearly zero. Since any small energy delivered to or taken from the localized particles at edge will move them either to conduction or valence band the position of localized edge states is the Fermi Level.

If the edge site has coordination number equal to one, the particle in it will be under only the exchange (hopping) strength in vertical direction and therefore the particle will has small probability to flow inside the zigzag stripe while the particle will have high probability to become localized in edge sites regardless its momentum q_x which then create an extended flat edge localized states at Fermi level.

Now we can use the elements of exchange matrix $T(q_x)$ and the Table I to understand the exchange (the hopping) flow of particles in armchair stripes. The diagonal elements are equal to $[(S J/2) \exp(-iq_x a)]$ while up and under elements are equal to $[(S J/2) \exp(-iq_x a/2)]$ which reflect that every site in one line of armchair stripe has only one nearest neighbor site in the same line, up line, and under line as seen in Figure 2, the half of up and under elements is due to the angle between up and under sites and the vertical of armchair lattice. The complex nature of armchair exchange matrix $T(q_x)$ elements show that the particle is forced to rotate from any armchair line to up or down lines due to the discontinuity in that lines. The particle in any interior site in the armchair stripe will be under three competitive exchange (hopping) force with different strengths: one strong through an armchair line along the translation symmetry of the stripe and the other two with equal less strength through up or down lines. Due to absence of armchair line contusions, the

particle flow pattern through armchair stripe will have interface effect [7] which lead to highest probability to hopping in aromatic cyclic chains with small interchain hopping probability [6, 9–14], and the number of those available complete aromatic cyclic chains depends on the the number of lines in the armchair. At the value of $q_x a/\pi$ between 0.25 and 0.5 the three exchange strength real part reach minimum and the imaginary part value reach maximum which mean that the particle will be nearly trapped inside an aromatic cycle, in this case high energy will be needed to move it to another aromatic cycle in the armchair stripe, which displayed as large band gap at the three armchair stripes.

While at $q_x a/\pi = 0.0$ the three exchange strength are nearly equal to pure real value which mean that the particle will be propagate inside an armchair line parallel to the direction of translation symmetry of armchair, to move the particle from armchair line in an aromatic cyclic chains to anther chain an energy will be needed which depend on the aromatic cyclic chains pattern guided by the texture of the ring currents under applying week magnetic field perpendicular to graphene nanoribbons shown in Figure 3 given in reference [7]. The Figure show that the armchair has three aromatic cyclic chains patterns for the three armchair types $3i$, $3i+1$, and $3i+2$. It is clear that the particle at armchair type $3i+2$ has great probability to tunnel from one chain to anther chain, since they are connected especially near the edge of the stripe which shown as touching between the conduction band and valence band at the Dirac point in the stripe dispersion relation. While the probability of tunneling of particle for the other two armchair types is neglected, and the particle need some energy to move from one chain to another chain which shown as two different band gaps between the conduction band and valence band the two stripes dispersion relations.

In armchair stripe there is only one kind of edge, where sites from sublattice A is connected with sites from sublattice B, those edge sites has only two coordination number, and the particle at those edge sites will be under only two exchange strength, which in that case are always not balance and consequently the particle will flow in edge armchair line parallel to the direction of translation symmetry of the stripe regardless its momentum q_x which explain the absence of flat localized edge states in armchair stripe.

The important difference between the particles exchange flow in zigzag and armchair stripes is the nature of flow as translation or rotational inside the stripe. While the exchange flow in zigzag stripes is a translation flow which shown in real nature of zigzag exchange matrix, the exchange flow in armchair stripes is a rotational which shown in complex nature of armchair exchange

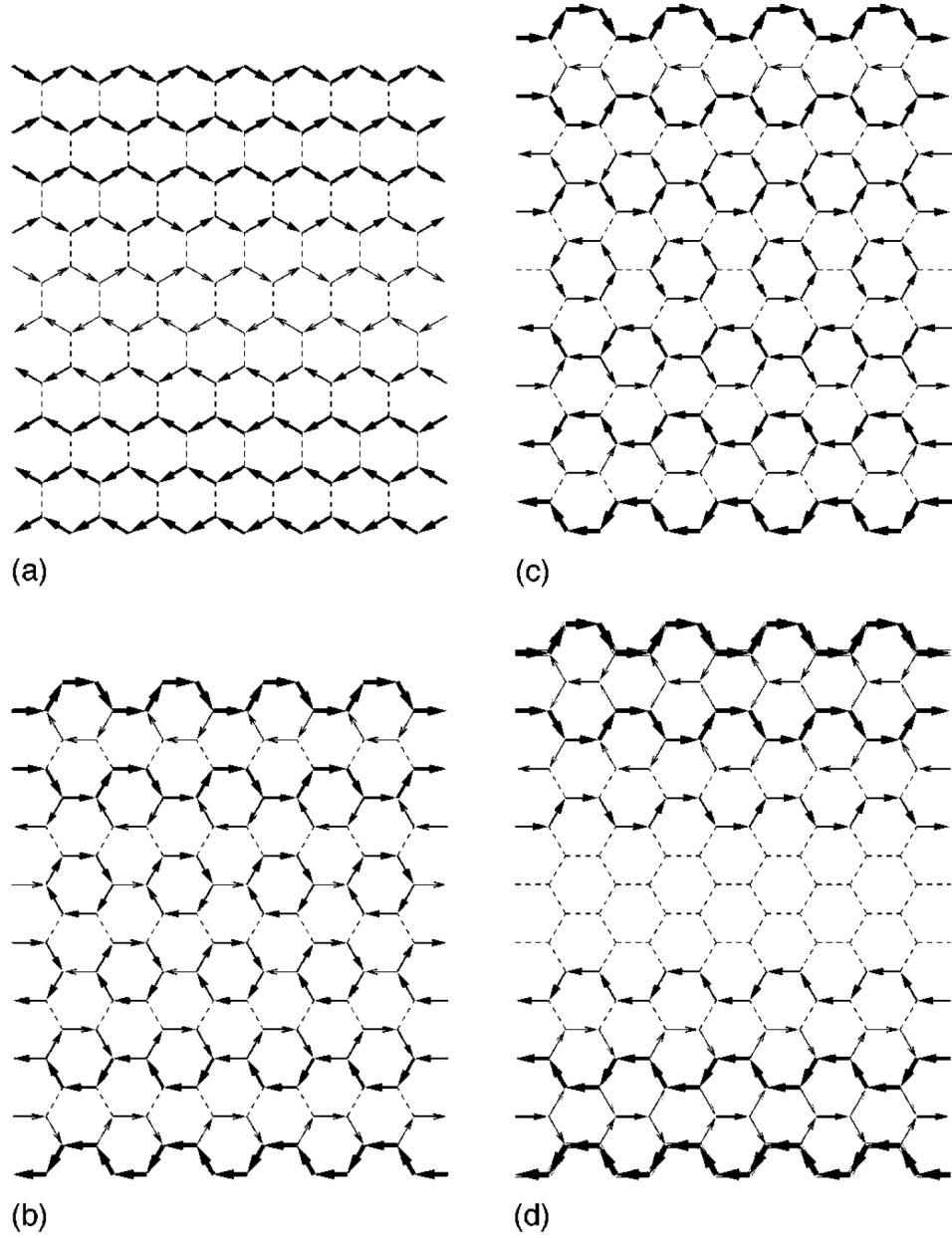


FIG. 3. The texture of the ring currents under applying weak magnetic field perpendicular to graphene nanoribbons for (a) zigzag ribbon ($N=10$) and armchair ribbons of (b) $N=18$, (c) $N=19$, and (d) $N=20$. In zigzag ribbon, because of the symmetry of the lattice, the ring currents along the vertical bonds are zero. In armchair ribbons of $N=18$ and 19 , the Kekulé pattern is clear. Figure and caption taken from [7].

matrix and clarified in the converting it to real equivalent matrix [1, 2]

$$\begin{bmatrix} \mathbf{Re}(q_x) & -\mathbf{Im}(q_x) \\ \mathbf{Im}(q_x) & \mathbf{Re}(q_x) \end{bmatrix}$$

where the real part sub matrix is equivalent to $\cos(\theta)$ function, and the imaginary part sub matrix is equivalent to $\sin(\theta)$ function and therefore it is no more than a rotation matrix with argument q_x . It is important to note that the flow in the extended graphene is similar to armchair stripe since the particles have a real angular momentum described by its pseudospin [15].

IV. APPLYING EXCHANGE MATRIX TO 2D SQUARE LATTICE

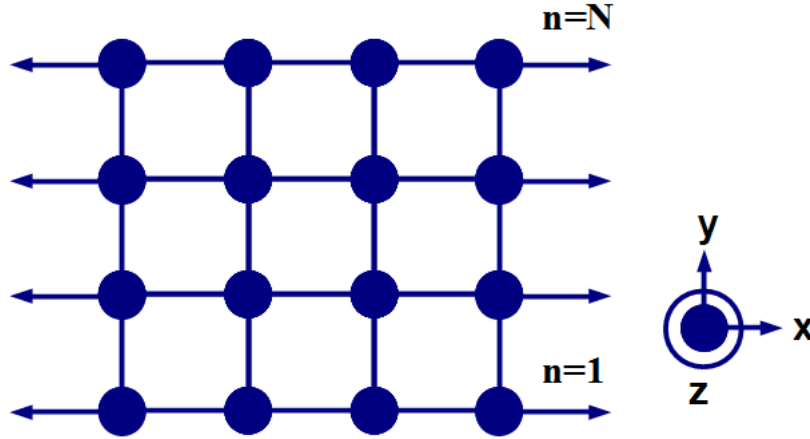


FIG. 4. Geometry of a 2D Heisenberg ferromagnetic square lattice nanoribbon. The spins are in the xy -plane and the average spin alignment is in z direction. The nanoribbon is finite in y direction with N atomic rows ($n = 1, \dots, N$).

Understanding the exchange matrix can help in the study of the 2D tight-binding and Heisenberg models for different 2D lattices configurations. The model easily explains the existence of flat band in 2D lattices and can be compared to other method [16]. We can apply the exchange matrix to 2D square lattice as following using figure 4 to identify the nearest neighbor connections for a site in 2D square lattice and applying to it the definition of exchange sum 4. The obtained exchange matrix for 2D square lattice is given in Table II, which is real matrix as expected from the square lattice geometry. Since the 2D square lattice is Bravais lattice there are only one lattice sites and therefore the \mathbf{E} matrix size is $N \times N$ and it is equal to summation of insite energy matrix

and the exchange matrix, i.e. $\mathbf{E} = \alpha I_N + T(q_x)$. Actually it is turn out that \mathbf{E} is the matrix obtained before for magnetic 2D square lattice using tridiagonal method [17].

TABLE II. Nearest neighbor exchange matrix elements for 2D square lattice

Parameter	Square lattice
β	$\frac{SJ}{2}$
ε	$\frac{SJ}{2}(2 \cos(q_x a))$
γ	$\frac{SJ}{2}$

Figure 5 shows the obtained spin wave dispersions for ferromagnetic 2D square lattice stripe with width $N = 8$. The right hand side is describing a magnetic stripe without impurities and with different edge exchange while the left side describes a magnetic stripe with an impurity line at line number 4 and with different impurity exchange. The figures show the unexpected feature of ferromagnetic 2D square lattice that the area and edge spin waves only exist as optic mode as seen before in [17], which now can be understand form the exchange matrix for 2D square lattice in Table II. The diagonal element $(SJ/2)(2 \cos(q_x a))$ shows that in 2D square lattice, the exchange strength for nearest neighbor between sites lies in the same line along the direction of translation symmetry of the stripe is larger compared by continues exchange strength for vertical nearest neighbor sites for most values of q_x . Since there is only one lattice sites type, the exchange flow in all lines is parallel and the main rule of the exchange in vertical nearest neighbor sites is to quantizing and reducing the energy as q_x decreases in every mode. Unlike the two sublattice zigzag case, there is no localized edge states at $q_x a / \pi = 0.5$ due to the absence of the two sublattice in the 2D square lattice and consequently its determinant depending on the exchange matrix $T(q_x)$ which lead to $\cos(q_x a)$ dependance of its modes dispersions.

Figure 5a shows the dispersion when the two edge exchange are equal to interior sites exchange, which for given material properties lead to absence of edge modes for the 2D square lattice, as the two edge exchange begin to decrease with respect to interior sites exchange, the strength for nearest neighbor exchange between sites lies along the edge begin to decreases which have more effect on particles with the low energy.

Figure 5b shows the effect of reducing edge exchange to half the value of the interior sites

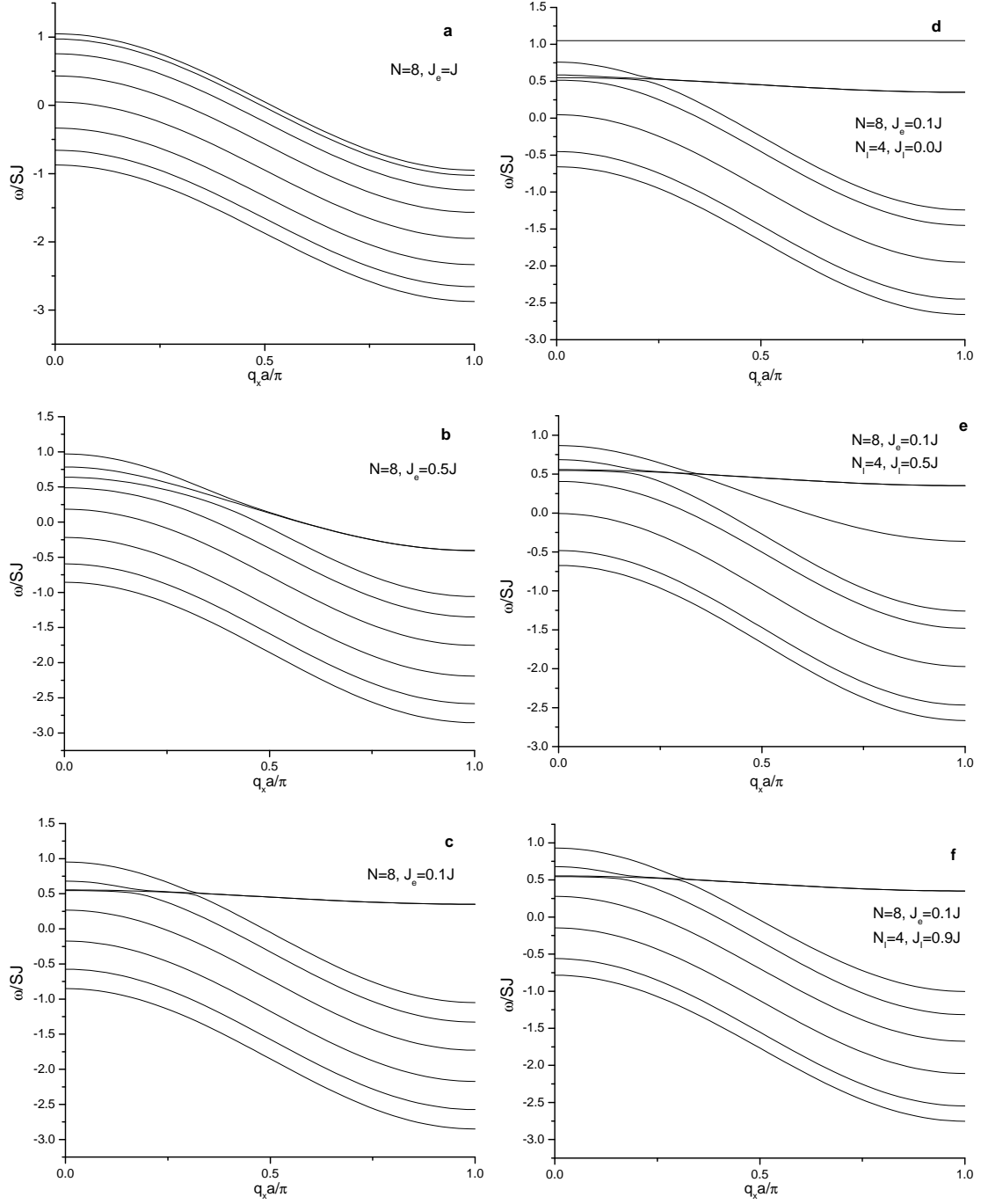


FIG. 5. Spin waves dispersion for ferromagnetic 2D square lattice stripe for $N = 8$ where $D = D_e = D_I = 1.0$ and $\alpha = -0.95$ (a) $J_e = J$ (b) $J_e = 0.5J$ (c) $J_e = 0.1J$. Adding an impurity line at line number 4 for $J_e = 0.1J$ with (d) $J_I = 0.0J$ (e) $J_I = 0.5J$ (f) $J_I = 0.9J$.

exchange. The particles with low energy become more localized on the edges, and less able to exchange with interior sites which make the two edges modes become degenerate and become outside the area modes boundary at low energy. While the particles with high energy still able to exchange with edge and interior sites, which show as no effect on the edges modes at high energy.

Figure 5c shows the effect of reducing edge exchange to 0.1 the value of the interior sites exchange. The particles with most q_x values become nearly localized on the edges, and almost not able to exchange with interior sites which make the two edges modes become flat degenerate outside the area modes boundary. The total energy of the two localized edges modes redistributed to equalize the particles energy residue on them, which lead to increase the energy of localized edges mode. The result is a large nearly flat edge mode, its energy are very near from high energy of the nearest neighbor upper and lower lines next to the edges and due to the coupling of the two edges with those two interior lines through vertical exchange, a resonance acquire between the edges flat mode and the high energy region of those two interior modes as seen in the figure. While the particles with high energy in edges modes are still able to exchange with edge and interior sites, which show as no effect on the edges modes at high energy.

Figure 5d shows the modified dispersion relations due to the effect of introducing substitutional a magnetic impurities line at row 4. The introducing of the impurities line have the effect as the case of zigzag stripes which is splitting the stripe to two interacted substripes with 3 lines and 4 lines. The strength of the interaction between the two sub stripes depend on the value of the impurities exchange value J_I , the Figure shows case when $J_I = 0$, in this case the expanded impurities flat localized states appear above the the area modes boundary. Those localized states are understood as accumulation sites for magnons in the interface created by the tunneling between the two substripes through the impurities line, and in the 2D square lattice only particles with highest energy will be able to tunnel through the impurities line, which shown as absence of highest energy mode form without impurities area modes.

Figure 5e shows the modified dispersion relations due to increasing of impurities lines exchange from zero to 0.5 from interior exchange, the Figure show that particles with high energy begin to flow between the two substripes and their energy mode part enter to the area modes boundary, while particles with low energy part from the impurity mode become localized flat branch outside the area modes.

Figure 5f shows the modified dispersion relations due to increasing of impurities lines exchange from 0.9 from interior exchange, the Figure show that particles with nearly all value of energy

begin to flow normally between the two substrips and their inter mode enter to the area modes boundary, i.e. the stripe become nearly without impurity

V. DISCUSSION AND CONCLUSIONS

In this work, a trial for understanding is done to the construction of exchange (hopping) matrix for short range (nearest neighbor) interaction by its lattice geometrical effect on particles flow (its topology).

This is used to explain the dispersion relations for 2D honeycomb lattice with zigzag and armchair edges obtained for graphene nanoribbons and magnetic stripes. The explanation shows the rule of zigzag edge geometry [18] in the appearance of peculiar localized edge states, and explain its absence in case of armchair edge configuration.

Using this understanding to construct the exchange matrix for 2D square Lattice and study the edge and impurities effects on its dispersion relations, the exchange matrix is used to give a physical interpretation for obtained results. The obtained results for 2D square Lattice using exchange matrix shows a similar behavior for its results obtained using the tridiagonal method discussed in [17].

Despite the fact that the exchange method gives very reasonable physical explanation for the 2D square Lattice results, the tridiagonal method has more advantage in study the edge effects and its energy states due to the separation of edges modes from area modes as shown in [17]. This shows the needs for study the edge states of 2D honeycomb lattice with zigzag edge using tridiagonal method, as it is done in [19].

ACKNOWLEDGMENTS

This research has been supported by the Egyptian Ministry of Higher Education and Scientific Research (MZA).

-
- [1] M. Z. Ahmed, *Study of electronic and magnetic excitations in the 2D materials represented by graphene and magnetic nano-ribbons*, Ph.D. thesis, The University of Western Ontario (2011), down-

load pdf version and a Viedo on Sciencestage.com.

- [2] M. Ahmed, (2011), arXiv:1110.5716v1 [cond-mat.mes-hall].
- [3] R. N. Costa Filho, G. A. Farias, and F. M. Peeters, Phys. Rev. B **76**, 193409 (2007).
- [4] A. H. Castro Neto, F. Guinea, N. M. R. Peres, K. S. Novoselov, and A. K. Geim, Rev. Mod. Phys. **81**, 109 (2009).
- [5] M. Müller, J. Schmalian, and L. Fritz, Phys. Rev. Lett. **103**, 025301 (2009).
- [6] M. Ezawa, Phys. Rev. B **73**, 045432 (2006).
- [7] K. Wakabayashi, M. Fujita, H. Ajiki, and M. Sigrist, Phys. Rev. B **59**, 8271 (1999).
- [8] J. R. M. Karim M. Abadir, *Matrix algebra*, Vol. 1 (Cambridge University Press, 2005).
- [9] K. Nakada, M. Fujita, G. Dresselhaus, and M. S. Dresselhaus, Phys. Rev. B **54**, 17954 (1996).
- [10] H. Zheng, Z. F. Wang, T. Luo, Q. W. Shi, and J. Chen, Phys. Rev. B **75**, 165414 (2007).
- [11] M. Fujita, K. Wakabayashi, K. Nakada, and K. Kusakabe, Journal of the Physical Society of Japan **65**, 1920 (1996).
- [12] S. Gopalan, T. M. Rice, and M. Sigrist, Phys. Rev. B **49**, 8901 (1994).
- [13] M. Fabrizio, A. Parola, and E. Tosatti, Phys. Rev. B **46**, 3159 (1992).
- [14] K. C. M. O. H. Hosoya, H. Kumazaki and Y.-D. Gao, Pure Appl. Chem. **62**, 445 (1990).
- [15] M. Mecklenburg and B. C. Regan, Phys. Rev. Lett. **106**, 116803 (2011).
- [16] K. Sun, Z. Gu, H. Katsura, and S. Das Sarma, Phys. Rev. Lett. **106**, 236803 (2011).
- [17] M. Ahmed, (2011), arXiv:1110.4369v1 [cond-mat.mes-hall].
- [18] C. Tao, L. Jiao, O. V. Yazyev, Y.-C. Chen, J. Feng, X. Zhang, R. B. Capaz, J. M. Tour, A. Zettl, S. G. Louie, H. Dai, and M. F. Crommie, Nat Phys **advance online publication**, (2011).
- [19] M. Ahmed, (2011), arXiv:1110.5105v1 [cond-mat.mes-hall].